

hood of 83°C. Below this temperature, the chain length decreased rapidly until approximately 310°K according to this model, thereafter decreasing more slowly. This calculation predicts that the average chain length should decrease by about an order of magnitude as the temperature goes from 331°K (58°C) to 311°K (38°C). In Table I, the shallow-trap density is seen to be greater by a factor of 40 in the sample prepared at 38°C over that prepared at 58°C. This suggests that the shallow traps are associated with the ends of chains, the length distribution of which is characteristic of the sample preparation temperature and is "frozen-in" at the temperature at which the measurements were made.

Amorphous selenium has many of the characteristics of a glass. In particular, selenium exhibits a glass transition temperature which may be associated with a second-order transition. For example, the slopes of the volume and entropy-temperature curves suffer a sharp decrease with decreasing temperature at the glass transition temperature T_g . For $T > T_g$, amorphous selenium is considered to be supercooled liquid, while for $T < T_g$, it is a glass. Eisenberg has determined $T_g = 31.0^\circ\text{C}$ for selenium for a study of its visco-elastic properties.

The physics of the glass transition is not completely

understood, but it is generally thought to involve a rapid change in the number of configurations available to the components of the glass (in this case, the selenium chain molecules). As the temperature decreases through T_g , the number of available configurations for the molecules should decrease abruptly. Hence, if a sample prepared at a temperature $T_1 > T_g$ is rapidly cooled below T_g , we would expect the chain-length distribution in the quenched sample to resemble closely that corresponding to the temperature T_1 . Our samples were cooled to room temperature in a matter of a few minutes after the completion of the evaporation, and all trapping measurements were made at temperatures $T < T_g$.

The decrease in shallow-trap density as the measuring temperature approaches the glass transition temperature may be understood in terms of the linking of chains. This shows up as an increase in the observed trapping time in Figs. 6, 7 and 8. As the temperature was raised, an increasing number of configurational degrees of freedom became available to the chain ends, improving the chances for linking up. This is to be expected from the increase in polymerization predicted by Eisenberg and the experimental observations of Briegleb and Richter and Herre.

Dynamics of Radiation Damage in Face-Centered-Cubic Alkali Halides

IAN McC. TORRENS AND LEWIS T. CHADDERTON

North American Aviation Science Center, Thousand Oaks, California

(Received 1 March 1967)

Computer simulations of ionic motion in 3-dimensional potassium chloride and sodium chloride crystals have been undertaken to investigate the effect of the regular lattice in influencing the energy spread in the crystal from a primary event such as might be caused by an incident energetic charged particle. Focusing of energy has been found to occur in several low-index crystallographic directions, including those where successive collisions involve oppositely charged ions. The neighboring assisting lines of ions exert considerable influence on the rate of energy loss along the focusing line, on the solid angle in which focusing occurs, and on the threshold energy for permanent ionic displacement from a lattice site, which was found to be a minimum of 25–30 eV in the (110) directions of potassium chloride. The feasibility of some mechanisms of F -center formation through ionic displacement is discussed in the light of this value of displacement threshold. The computations reveal a new concept of focusing, for which there is a *lower* energy limit for propagation of a focuson. This limit can be as high as several hundred electron volts for higher-order focusing through asymmetric assisting ionic "lenses." At energies above the lower focusing-energy limit, the momentum transfer of the moving ion to its neighbors between focusing collisions is sufficiently small compared to its forward momentum for its trajectory to be altered only slightly by collision with different parts of the assisting lens. At lower energies, asymmetric collisions with lens ions result in defocusing.

I. INTRODUCTION

IN the past few years the influences of the crystal lattice on the motion of energetic charged particles and on the dissipation of energy in a crystalline material during irradiation have become topics of major interest to investigators of radiation damage in the solid state. Anisotropy of the lattice has the effect of enhancing

the processes of energy transfer in some crystalline directions over that which we might expect if the atoms of the irradiated material were randomly distributed in the solid. An important example of this is the phenomenon of *focusing*,^{1,2} in which energy is transferred

¹ R. H. Silsbee, *J. Appl. Phys.* **28**, 1246 (1957).

² M. W. Thompson and R. S. Nelson, *Proc. Roy. Soc. (London)* **A259**, 458 (1961).

by sequences of atomic collisions along lines of atoms in low-index crystallographic directions. Another directional effect occurs when an atom or charged particle passes between rows or planes of atoms in the crystal, experiencing only glancing collisions, so that there is an anomalously low rate of energy loss and a greatly increased range. This phenomenon is known as channeling.³⁻⁵ The net result of both these processes, however, is the transmission of energy and, in the case of channeling, momentum (and therefore mass) from the immediate region of a primary collision event. The severity of any localized damage is therefore reduced by efficient mechanisms of energy removal away from the thermal/displacement volume.

One method of investigation of directional effects in a crystal lattice, which is theoretical in basis though largely experimental in technique, is computer simulation of the dynamic motions of atoms in a crystallite during a damage event, a method initially developed by Gibson, Goland, Milgram, and Vineyard⁶ at Brookhaven National Laboratory. This involves applying an iterative procedure and the classical laws of motion to calculate atomic trajectories in the simulated crystal-line array. It has the advantage that, while most analytical calculations consider only two-body atomic collisions, the computer simultaneously can take into account the interaction of colliding atoms with each other and with neighboring atoms of the crystal.

Using this technique, Vineyard and co-workers have investigated low-energy dynamic events in face-centered-cubic (fcc) copper and have shown that focusing of energy can occur with high efficiency in some low-index crystal directions. The work has been subsequently extended by Erginsoy⁷ to body-centered-cubic (bcc) iron. Other investigators have used similar simulation methods to study both focusing and channeling in a number of metals and alloys,⁸⁻¹⁰ and it is desirable to extend the technique, if this is feasible, and a realistic model can be presented, to other types of crystal lattices. Our particular interest in this connection has been with fcc ionic crystals, since many theories of color-center defect formation involve the motion and displacement of lattice ions following irradiation, and since the lattice is pseudo-simple-cubic, so that new directional effects should be in evidence. The binding, moreover, is ionic, and the interatomic potential contains a long-range electrostatic

contribution in addition to the short-range closed-shell repulsion. The discrepancy between ionic sizes and masses in an alkali halide should also affect the energy loss from a primary event and have a marked influence on focusing phenomena.

Extension of the computer simulation technique to alkali-halide lattices has accordingly been initiated in order to obtain information about ionic motion and anisotropic directional effects in these structures. Preliminary results have been reported previously.¹¹⁻¹³

II. COMPUTATIONAL PROCEDURE

The structures which have been studied to date are those of potassium chloride, in which the alkali and halide ions are similar in size, and sodium chloride, for which there is an approximately two-to-one ratio in ionic size. Both structures are strictly fcc, but may be "constructed" by arranging alternately the anions and cations on the lattice points of a simple cubic lattice. Potassium chloride has a lattice parameter of 3.14 Å, sodium chloride, 2.81 Å. Some principal crystallographic directions in a potassium, chloride lattice are shown in Fig. 1.

An fcc section of an infinite crystal was simulated in the machine and one ion was given a selected kinetic energy as though struck by an incoming particle. The computer then employed the classical equations of motion and a central-difference procedure to find the positions and velocities of the ion at the end of consecutive equal intervals of time. The same procedure was followed for the neighboring ions with which the "knock-on" interacted and the disturbance was traced as it spread through the crystallite.

If M is the mass of the ion, $x_i(t)$ and $v_i(t)$ are the i th atomic coordinates and velocities, respectively, at time t , and F_i is the force on the atom due to its interaction

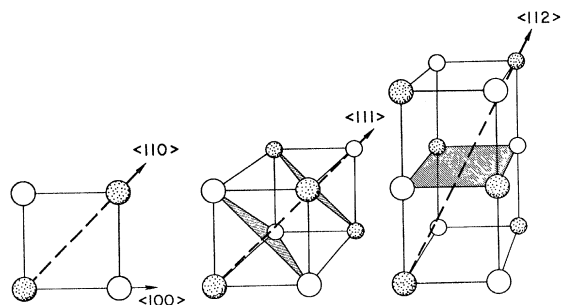


FIG. 1. Principal crystallographic directions in potassium chloride. Shaded areas show "ionic lenses" through which focusers in $\langle 111 \rangle$ and $\langle 112 \rangle$ directions must pass.

³ C. Lehmann and G. Leibfried, *J. Appl. Phys.* **34**, 2821 (1963).

⁴ E. Bøgh, J. A. Davies, and K. O. Nielsen, *Phys. Letters* **12**, 129 (1964).

⁵ J. Lindhard, *Kgl. Danske Videnskab. Selskab, Mat.-Fys. Medd.* **34**, No. 14 (1965).

⁶ J. B. Gibson, A. N. Goland, M. Milgram, and G. H. Vineyard, *Phys. Rev.* **120**, 1229 (1960).

⁷ C. Erginsoy, G. H. Vineyard, and A. Englert, *Phys. Rev.* **133**, A595 (1964).

⁸ J. R. Beeler, Jr., and D. G. Besco, *Radiation Damage in Solids* (International Atomic Energy Agency, Vienna, 1962), p. 43.

⁹ W. L. Gay and D. E. Harrison, Jr., *Phys. Rev.* **135**, A1870 (1964).

¹⁰ M. T. Robinson and O. S. Oen, *Phys. Rev.* **132**, 2385 (1963).

¹¹ L. T. Chadderton and I. McC. Torrens, *Nature* **208**, 880 (1965).

¹² L. T. Chadderton, D. V. Morgan, and I. McC. Torrens, *Phys. Letters* **20**, 329 (1966).

¹³ I. McC. Torrens, L. T. Chadderton, and D. V. Morgan, *J. Appl. Phys.* **37**, 2395 (1966).

TABLE I. Computational units for potassium and sodium chlorides.

Unit	KCl	NaCl
Length	3.14×10^{-8} cm	2.81×10^{-8} cm
Time	4.47×10^{-16} sec	3.07×10^{-16} sec
Mass	3.25×10^{-26} g	1.91×10^{-26} g
Energy	For both 1.602×10^{-12} erg = 1 eV	
Velocity	7.025×10^6 cm/sec	9.16×10^6 cm/sec

with its neighbors, then the equation of motion is

$$\dot{v}_i(t) = (1/M)F_i. \quad (1)$$

In the case where the force on an ion on the boundary of the crystallite is being considered, F_i depends on the velocity as well as on position. The boundary forces therefore consist of a viscous damping force and a Hooke's-law restoring force, the combination being a reasonable approximation to the effect of an infinite crystal extending beyond the edge of the crystallite. From Eq. (1), approximating by finite differences,

$$v_i(t + \frac{1}{2}\Delta t) = v_i(t - \frac{1}{2}\Delta t) + (\Delta t/M)F_i, \quad (2)$$

$$x_i(t + \Delta t) = x_i(t) + \Delta t v_i(t + \frac{1}{2}\Delta t), \quad (3)$$

where Δt is a small time interval. Thus, by knowing all velocities $v_i(t - \frac{1}{2}\Delta t)$ and positions $x_i(t)$, and by calculating the interionic forces F_i , the new positions and velocities at a time Δt later can be computed. These values were taken as initial values for the next time step, and so on.

The choice of the time interval Δt depended on exacting a compromise between the approach to an analytically accurate calculation and the computational time required for such a calculation. Normally a value was chosen so that further reduction made no significant difference to the ionic trajectories during a damage event. Checks on energy conservation were incorporated into the program.

For convenience in calculation and in analysis of the results, fundamental units of similar significance to those of Gibson *et al.*⁶ were selected. These were slightly different for potassium and sodium chlorides, and are shown in Table I.

The crystallite of the simulation contained 1000 ions in a $10 \times 10 \times 10$ cubic array with $\{100\}$ faces. The input routine allowed any number of ions to be set moving initially with stipulated energies, and ions could be placed in nonlattice positions. Since only elastic energy losses were considered and no electronic interactions were allowed, the initial energy in all cases did not exceed 1000 eV. In this region electronic energy losses were assumed to be small enough to be neglected.

III. INTERIONIC POTENTIALS

For an ionic crystal, it is a basic assumption that the solid may be considered as a system of positive and negative ions, the force between two such ions depending

only on their distance apart and having no directional variation. This interaction has two components: the electrostatic force which is repulsive or attractive, depending on whether the interacting ions are of the same or opposite charge, and the repulsive force due to the overlap of the closed electron shells of neighboring ions.

For a two-body interaction, two main forms of repulsive potential have been used¹⁴⁻¹⁷:

$$V(r)_{\text{repulsive}} = \lambda/r^n, \quad (4)$$

$$V(r)_{\text{repulsive}} = A \exp(-Br). \quad (5)$$

The inverse n th power potential is empirical, while the Born-Mayer exponential form is based on a calculated statistical electron-density distribution in the ion. The former increases rapidly to infinity with decreasing values of r , whereas the Born-Mayer exponential approaches a finite limit as r approaches zero (Fig. 2). In the region of r in which these potentials are most accurate, near the equilibrium position, they are both sufficiently small in comparison to the electrostatic term for their difference to be insignificant. The inverse n th power potential is, in our view, the more accurate in the region of interaction which is of most interest in dynamic events (up to a few hundred electron volts). Events run with both potentials in this energy regime produce results which we believe substantiate this conclusion. There are two generally accepted methods of assigning a value to the index n . Some investigators have used the potential which has become known as the Born-Mayer-Verwey potential following a treatment by Verwey of the ionic-shell repulsion in the molecule.¹⁶ In this, a value of 12 is derived for the index n . This, however, is somewhat too hard for dynamic motion of the ions, where the interionic distance is often considerably less than the equilibrium distance in the crystal. In addition, it emerges

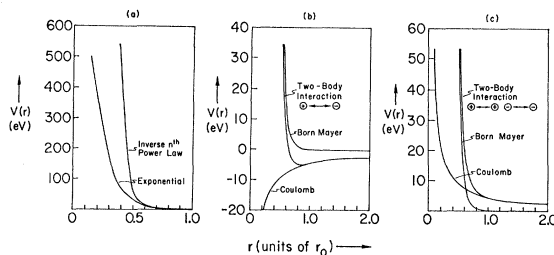


Fig. 2. Interionic potentials in potassium chloride. (a) Comparison of Born-Mayer exponential and inverse n th power form of the repulsive potential; (b) and (c), computational potentials in KCl, with their repulsive and Coulomb components.

¹⁴ L. Pauling, *The Nature of the Chemical Bond* (Cornell University Press, Ithaca, New York, 1939).

¹⁵ M. Born and M. Goepfert-Mayer, in *Handbuch der Physik*, edited by S. Flügge (Julius Springer-Verlag, Berlin, 1933), Vol. 24, p. 633.

¹⁶ E. J. W. Verwey, *Rec. Trav. Chim.* **65**, 521 (1946).

¹⁷ F. G. Fumi and M. P. Tosi, *J. Phys. Chem. Solids* **25**, 31 (1964); **25**, 45 (1964).

from a consideration of the repulsive interaction in a single molecule rather than in the crystal. A more reasonable potential for our purpose is the Pauling form,¹⁴ where the value of n depends on the closed-shell ion size, being 9 for K^+-K^+ , K^+-Cl^- , and $Cl^- - Cl^-$ interactions, 8 for Na^+-Cl^- , and 7 for Na^+-Na^+ . Thus, the potential is slightly softer for the smaller ions. The value of λ in each case was found from a consideration of the equilibrium ionic configuration in the crystal. However, in the case of NaCl the potential constants for the identical ion interactions were adjusted for ionic size.

The electrostatic term of the potential was of the form

$$V(r)_{\text{electrostatic}} = e^2_{\text{eff}} / \epsilon r, \quad (6)$$

where e^2_{eff} was 0.5 for KCl and 0.64 for NaCl, e being the electronic charge. The ϵ represented a dielectric reduction which was 1 for interaction with nearest neighbors, and 2 for next-nearest neighbors and greater.¹⁸ These reductions to the basic Coulomb potential made some allowance for polarization of the ions, and for electronic screening.

The final potentials used in the computation are shown in Fig. 2. The electrostatic term of the potential is considerably larger than the ion-shell repulsion at distances in the region of and greater than the equilibrium separation of the ions in the crystal, and is thus more influential for long-range interactions.

It is important at this point to stress that in utilizing the computer-simulation technique we are not seeking accurate quantitative results. We are endeavoring, rather, to obtain a better qualitative understanding of those phenomena which are related to ionic motions in crystals such as the alkali halides, than we should achieve by either analytical calculation or simple empirical considerations alone. We also believe that the potentials which have been employed are reasonable, first of all since they are based on established theories of binding in ionic crystals, and secondly since the effects of altering them within reasonable limits and of trying different accepted analytical forms have only a trivial effect on the general progress of a damage event.

Another observation which should be clearly stated here is that, in a perfect crystal, the effect of cutting off the potential between two ions at a separation of $3r_0$ (r_0 =equilibrium $\langle 100 \rangle$ lattice spacing) is negligible for events in the dynamic energy range. Again, detailed numerical results are altered, but the general conclusions for a particular event remain substantially the same.

IV. RESULTS

A. Focusing in the $\{100\}$ Planes

Interpretation of computer-simulation results requires considerable care, especially in the extrapolation

of results from the model to the solid. We shall see later, however, that the $\langle 110 \rangle$ directions play a dominant part in many low-energy displacement and sub-displacement events, and for this reason we present in this section some discussion of events initiated entirely in a $\{100\}$ plane. It is clear, of course, that an ion moving in such a plane may well be in a state of unstable equilibrium. Only a small component of motion out of the plane—easily supplied by the vibrating lattice—may be necessary to send the ion into the third dimension and to absorb the excitation more rapidly. Yet the behavior of ions neighboring the knock-on, the efficiency of focusing down the like-ionic $\langle 110 \rangle$ directions, and the observation that an allowed relaxation of neighboring $\{100\}$ planes does not alter the course of a typical event, prompt us to present the results in the way we have chosen.

1. Ionic-Lens Anomalous Effects

The results of some events run in potassium chloride are shown in Figs. 3–6. In the event depicted in Fig. 3, a potassium ion was given an energy of 80 eV and was projected in a direction making an angle of $\tan^{-1} 3/2$ with a $[100]$ direction (that is, at about 11.3° to a $[110]$ line). This resulted in a strongly assisted focusing of energy down the $[110]$ line, in which each succeeding ion of the sequence was deflected by a single “ionic lens” consisting of two chlorine ions, so that it subsequently made an almost head-on collision with the next ion in the line. While the initial ion succeeded

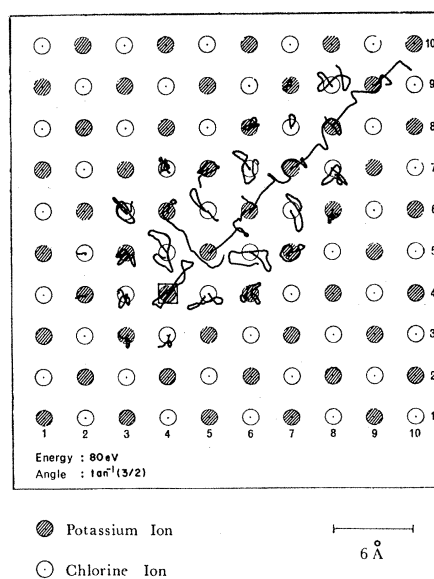


FIG. 3. Progress of a displacement event in which a potassium ion (boxed) receives energy 80 eV and moves off at about 11.3° to $[100]$. Focusing occurs strongly in the $[110]$ direction, removing over half of the initial energy from the array. A sequence of replacements occurs along the line, and a possible final configuration is an interstitial somewhere outside the array, and a vacancy in the immediate vicinity of the primary event.

¹⁸ B. Szegedi, *Trans. Faraday Soc.* **45**, 155 (1949).

in crossing back through the potential barrier and eventually in returning to its original position in the lattice, the subsequent ions in the focusing line were forced to replace sequentially. The "simple lens" analogy will not predict this behavior. The ionic lens must be permitted to move and vary in strength under the influence of the passing ion, becoming astigmatic with a time-dependent focal length. Thus the returning knock-on found that the assisting lens, after a temporary disturbance, had reformed in a position where it aided a return to the original lattice site. Subsequent ions of the sequence were forced into replacement sites by their reconstituted potential barriers. It is suggested, therefore, that the reason for the anomalous behavior of the knock-on is the fact that it received its energy instantaneously, on its lattice site, while subsequent ions were *gradually* accelerated from rest during the collision time. The resulting difference in the disturbance of the ions of the lens was sufficient to cause permanent displacement in the secondary cases, and the return of the primary to its lattice site. This type of damage trajectory pattern has been observed in a large number of events with varying initial energy and angle of projection of the primary ion.

Another manifestation of an anomalous lens effect may be seen in the probable final configuration of this event. It seems that a vacancy will be left, not in the $[110]$ line of the focusing sequence, but in a neighboring $[110]$ potassium line, the ion diffusing from its site through a temporarily absent barrier into the line of the focusing sequence. The $[110]$ dynamic crowdion will in all probability be terminated by an interstitial crowdion configuration after a number of further focusing collisions. This type of crowdion configuration has been shown to be stable in a separate run (Fig. 4). For this event a potassium ion in a large array was set moving with an energy of 30 eV at 5° to the $[110]$ line. The final configuration consisted of a vacancy in the place of the second ion, with a stable $[110]$ crowdion some six $[110]$ lattice distances from the original knock-on. During the propagation of the dynamic

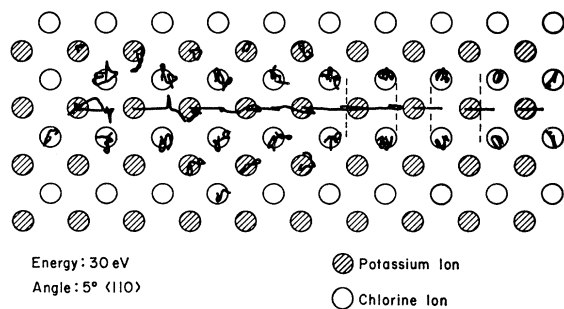


FIG. 4. Degradation of a dynamic into a static crowdion. The potassium ion receives an energy of 30 eV at 5° to $[110]$, resulting in the production of a symmetrical crowdion interstitial on the $[110]$ line six lattice spacings away. A perfect focuson travels on out of the set.

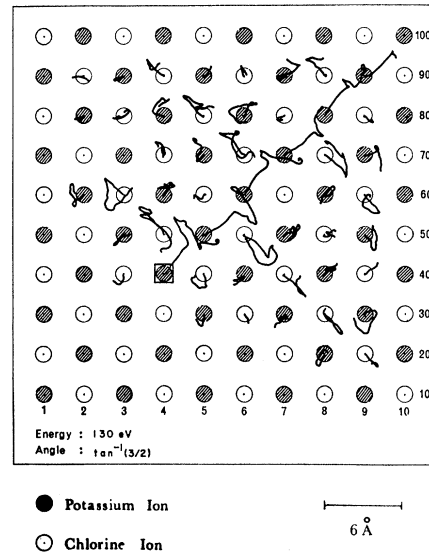


FIG. 5. An event similar to that of Fig. 3, with the initial energy raised to 130 eV. Now the first ion also is displaced, and we note that secondary $[110]$ focusing is commencing at 90° to the main sequence.

crowdion the ions in the immediately neighboring $[110]$ chlorine rows relaxed in such a way that a wave of charge polarization followed the propagation of the sequence through the lattice. The configuration of the static crowdion was symmetrical with respect to the lattice site, and the neighbors in the $[110]$ line came to equilibrium in positions displaced outward along $[110]$ from the original lattice sites.

An event identical to that of Fig. 3, with the exception

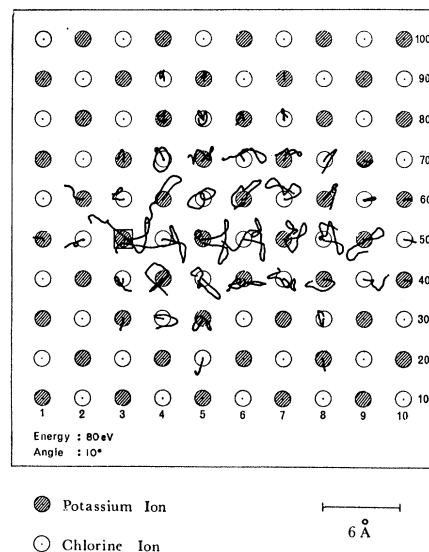


FIG. 6. The initial direction of motion of the struck potassium ion is in this case at 10° to $[100]$, illustrating the relatively inefficient simple focusing process. No $[100]$ replacement occurs, being energetically unfavorable in lines of alternately oppositely charged ions.

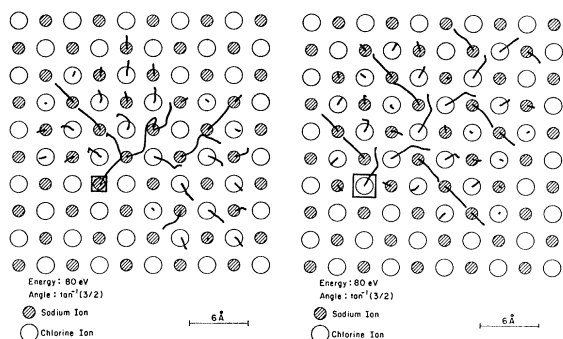


FIG. 7. Events with the initial conditions of that of Fig. 3 for Na^+ and Cl^- ions in sodium chloride. Focusing is less efficient because of the size discrepancy of the ions in this lattice. Subsidiary $[110]$ focusons are generated in the Cl^- event, and an interesting effect in the Na^+ focuson is its removal through interaction with a Cl^- lens ion to the neighboring parallel Na^+ $[110]$ line.

that the initial potassium ion energy has been raised to 130 eV, is depicted in Fig. 5. In this case the energy was sufficiently high for the first ion to replace. Also of note in this event are the secondary $[110]$ chlorine ion focusing chains at 90° to the main sequence, which were influential in efficiently removing energy from the principal focusing line. The course of a further event involving an 80-eV potassium ion, this time traveling initially at 10° to $[100]$ is portrayed in Fig. 6. The energy became focused along $[100]$ but through lack of any assistance from adjacent lines the efficiency was considerably less. Replacement of unlike ions in $[100]$ focusing was not expected and did not occur at energies of this order, due to the absence of an assisting potential barrier.

The dynamic motion of ions in the *sodium chloride* lattice was influenced by the discrepancy in ion size of the Na^+ and Cl^- ions. The focusing efficiency was consequently less and the replacement characteristics were also somewhat different from those for KCl. Figure 7 shows the $\langle 110 \rangle$ focusing in events where sodium and chlorine ions were projected, again at 11.3° to $[110]$, with 80 eV of kinetic energy. In the event where the chlorine ion was initially projected, a replacement sequence ensues, similar to that for KCl. Sodium-ion focusing appeared different, in that the effect of collisions of the small ion with the large chlorine-ion lenses was sufficiently severe to cause rapid defocusing in the original $[110]$ line, although subsidiary focusons developed in other $\langle 110 \rangle$ sodium lines.

2. Focuson Propagation and Energy Loss

The consequences of the differences in trajectory of identical events run in NaCl with Na^+ and Cl^- ion focusing, and in KCl with K^+ ion focusing may be illustrated by reference to plots of energy as a function of time for focusons with initial energies of 30 and 80 eV. Thus, in Fig. 8 the maxima of the kinetic-energy curves for successive ions of the focusing line are con-

sidered to be representative of the transmitted focuson energy.

It is clear from the shape of the uppermost parts of the energy curves that the chlorine ions experience very little detectable influence of the lenses, whereas the others, in differing degrees, are sensitive to the barriers. The general pattern for focuson propagation in the $\langle 110 \rangle$ directions is an initial drop in energy over the first one or two collisions, being the more pronounced the further off-axis the initial direction of motion, followed by an almost constant energy loss as the focuson is attenuated, though the rate of energy loss does in fact decrease slightly as the energy drops. In all of these plots diffusive relaxation motion of individual ions has been neglected since it has no major effect on the propagation of the focuson.

3. Efficiency of Low-Index Focusing: Energy-Correlation Diagrams

We may illustrate schematically the relative importance of the main directions in a $\{100\}$ plane as regards the efficiency of focusing by a technique involving superposition of trajectories of events where the primary ion has always the same energy, and its initial direction of motion is varied through 360° in angular increments of 5° or 10° . Such diagrams, which we term *energy-correlation* diagrams, can be plotted for any crystal plane and supply information regarding the importance of anisotropic effects in the lattice of the simulation.

The 80-eV correlation diagram for a struck potassium ion in KCl is illustrated in Fig. 9, and the relative importance of certain crystallographic directions in the focusing of energy away from a primary event becomes immediately evident. In particular, the $\langle 110 \rangle$ assisted focusing is extremely predominant and much more intense than the $\langle 100 \rangle$ focusing.

Some other facts come to light through this type of orbit diagram:

1. The size of the affected region is governed by the energy of the knock-on, and the disturbance is generally

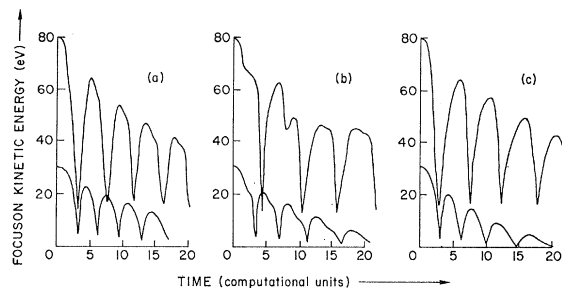


FIG. 8. Kinetic-energy curves for ions of 80 and 30 eV $\langle 110 \rangle$ focusons: (a) K^+ in KCl, (b) Na^+ in NaCl, and (c) Cl^- in NaCl. An initial sharp drop in focuson energy occurs over the first one or two collisions, followed by a more constant rate of energy loss as the ionic trajectories approach the axis of focusing.

concentrated along or near to the principal focusing axes.

2. The disturbance of the $\langle 100 \rangle$ lenses by the traversal of the focuson is clearly illustrated.

3. The fact that the lattice is tightly bound is made evident by the absence of trajectories of neighboring ions which touch or cross.

4. The symmetry of the spread of the damage region is very pronounced.

Similar correlation diagrams for Na^+ and Cl^- primaries in sodium chloride are shown in Fig. 10, though the computation time for these was larger than in Fig. 9. The effect of the different ion size is immediately obvious. Much more overlapping of trajectories occurs in the sodium case, the center of the pattern having only small "forbidden areas" free of trajectories. Also noticeable is the greater disturbance of the lenses for the chlorine primary and the higher degree of focusing in the sodium $\langle 110 \rangle$ sequences.

B. Focusing in the $\langle 111 \rangle$ Directions

The $\langle 111 \rangle$ direction in a cubic crystal is interesting from the point of view of focusing, since between each collision there are two triangular lenses of ions to be traversed (Fig. 1). In an alkali halide, moreover, the direction is particularly interesting since the ions in the focusing line are alternately alkali and halide ions, and the two assisting lenses each consist of three ions of identical type. This affords an opportunity to study the transmission of energy through focusing in a doubly assisted chain.

Investigation of $\langle 111 \rangle$ focusing was carried out for different initial energies and directions of motion as in a $\{100\}$ plane. In general, the advantages of pronounced assisted focusing were counteracted, especially in low-

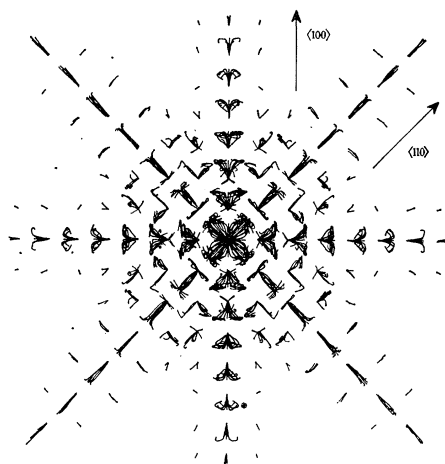


FIG. 9. 80-eV energy-correlation diagram for a struck potassium ion in a $\{100\}$ plane of potassium chloride. The diagram is built up from the superimposed trajectories of events in which the initial direction of motion is varied through 360° . The predominance of $\langle 110 \rangle$ focusing and the effect of the ionic lenses is clearly illustrated.

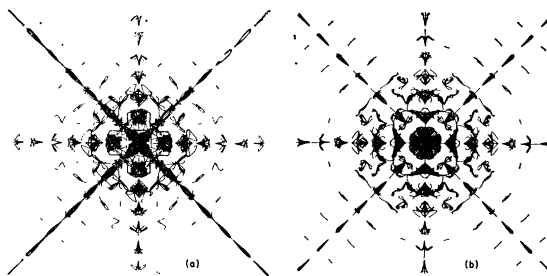


FIG. 10. Energy-correlation diagrams for 80-eV primary knock-ons in sodium chloride: (a) Na^+ , (b) Cl^- . Much more overlapping of trajectories occurs in the sodium-ion case, and a greater disturbance of the lenses characterizes the chlorine-ion diagram.

energy events, by energy losses of the focuson to the lenses. This may be illustrated by reference to the ion energy curves for 30 and 80 eV focusons in this direction (Fig. 11).

In all cases (K^+ in KCl , Na^+ and Cl^- in NaCl) the range was much less than that for a 30-eV focuson in $\langle 110 \rangle$ $\{100\}$. The curves reveal very clearly the action of the lenses, the critical factor being the amount of energy lost by one ion of the sequence before the next ion begins to move. For example, in sodium chloride, when a chlorine ion of 30 eV initiates the sequence, the next ion in the $[111]$ line, a sodium, receives only about 5-eV maximum kinetic energy and the disturbance fails to penetrate the next chlorine lens. A further significant point is that the energy lost to the two lenses is generally funneled off in both structures down $\langle 110 \rangle$ directions as long-range focusons, thus confirming the vital importance of $\langle 110 \rangle$ focusing in these lattices.

Variation of the focuson energy up to 500 eV in potassium chloride confirmed that $\langle 111 \rangle$ is indeed a good focusing direction in this compound, the energy loss per focusing collision distance being approximately 10 eV for ions traveling directly along the axis.

C. Higher-Order Focusing: The $\langle 112 \rangle$ Directions

The $\langle 112 \rangle$ directions, and other higher-index directions in the crystal, are somewhat different from those

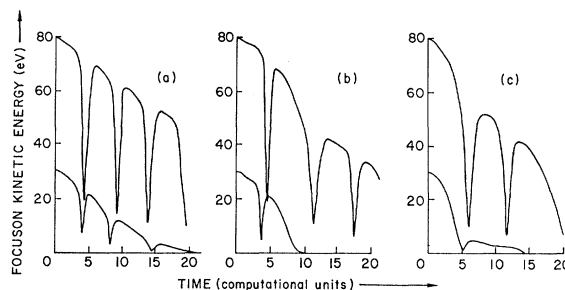


FIG. 11. Kinetic-energy curves for the ions in 30-eV and 80-eV axial $\langle 111 \rangle$ focusons: (a) K^+ in KCl , (b) Na^+ in NaCl , (c) Cl^- in NaCl . Much more energy is lost to the lens ions than in the $\langle 110 \rangle$ case, and in NaCl the ion size difference along the $\langle 111 \rangle$ line further reduces the focusing efficiency.

which we have so far discussed. The assisting potential barrier is, in the $\langle 112 \rangle$ case, an asymmetric lens consisting of four ions of a $\{100\}$ plane, and the distance between focusing collisions is some 2.45 lattice spacings. Consequently, we expect much more critical conditions for the initial energy and direction of motion to prevail if focusing is to occur.

This is indeed the case for normal focusing energies. However, events run in this direction have demonstrated a new concept of assisted focusing in which the phenomenon is rendered possible by a situation similar to that which is assumed in analytical momentum approximation calculations. For initial energies up to over 100 eV, no focusing occurs, and the trajectory of the first ion traveling in a $[112]$ direction is so modified by collision with its neighbors that it collides almost head-on with a $[111]$ neighbor. For a 200-eV ion, less deviation from the initial trajectory results from the collision with the neighbors, and the initial ion then collides with its neighbor in the $[112]$ direction, which receives 100 eV. The sequence of collisions is illustrated in the kinetic-energy plot of Fig. 12, for focusons of 200 and 500 eV. The trajectory of the 500-eV ion is scarcely affected by collision with its $[001]$ and $[111]$ neighbors, as can be seen in the shapes of the kinetic-energy peaks, and it goes on to give up almost all of its energy to the next ion of the $[112]$ line.

Thus, events run in a $\langle 112 \rangle$ direction reveal a *lower* energy limit for focusing, dependent not, as in the $\langle 111 \rangle$ focusing, on the ability of the energetic ion to penetrate the assisting lens, but on the ability of the ions of an asymmetric lens to modify the trajectory of the traversing ion, thereby terminating the focuson. It is perhaps

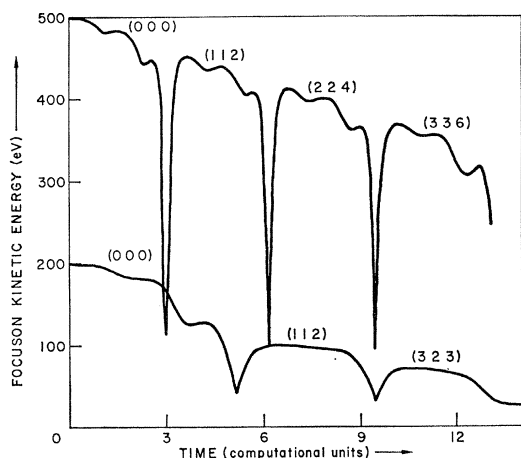


FIG. 12. Kinetic energy for "impulse" focusing in the $[112]$ direction, at 200 and 500 eV initial energy. The former survives only one focusing collision, degenerating into a $[111]$ focuson, but as the energy is increased the trajectory is only slightly modified by collisions with the asymmetric lens, and the focuson survives several collisions. The effect of collisions with the lens ions is demonstrated by the shape of the energy maxima of the separate ions. Numbers in brackets refer the position coordinates of ions whose energy is plotted to the initially struck ion as origin.

more correct to call this particular phenomenon "hindered" rather than assisted focusing, and we believe that in view of the rather critical conditions required for the direction of motion of the first ion, focusing in this direction in KCl-type alkali-halide lattices will necessarily be inefficient. The same argument of course applies to higher-order focusing.

In the case of the sodium ion of sodium chloride another possibility arises from the comparatively small size of this ion. A sodium ion moving in the $[112]$ direction with an energy of 80 eV, as a result of a collision with a neighboring chlorine ion, is deflected in such a way that it moves into a field of low-interaction potential between adjacent $[001]$ rows of ions, becoming effectively axially channeled. Simultaneously, a $[111]$ chlorine focuson initiated by the first collision rapidly degenerates into a $[110]$ focuson, and both focuson and channelon persist until the termination of the computation of the event (Fig. 13). This once

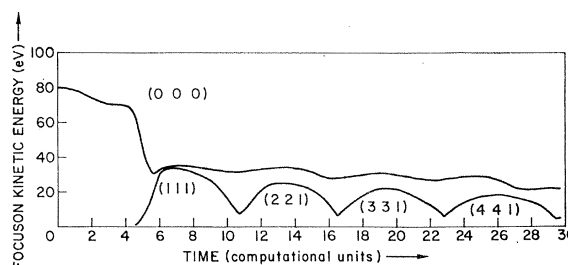


FIG. 13. A sodium ion set moving with energy 80 eV in the $[112]$ direction becomes channeled between $[001]$ lines of ions as a result of its collision with the nearest neighbor in the $[111]$ direction. The energy-time curve shows the resulting simultaneous propagation of the channelon and a $[110]$ focuson. Numbers in brackets have similar significance to those of Fig. 12.

again indicates the relative importance of the $\langle 110 \rangle$ axes as fundamental directions for energy dissipation by focusing mechanisms, and confirms that in diatomic solids in which one atomic specie is considerably smaller than the other, there is a finite probability of the far transfer of both mass and energy from the primary event.

D. The Ionic Displacement Threshold

Many of the primary damaging events which were simulated culminated frequently in defect configurations which typically comprised several ionic replacements to substitutional sites and one permanent *displacement* to an interstitial site. It was logical, therefore, to ask how the displacement threshold E_d , the minimum knock-on energy required for the introduction of a permanent Frenkel pair, varied with the initial direction of projection. In particular, since there is a marked effect of assisting ionic lenses in $\langle 110 \rangle$ displacements events in $\{100\}$ planes, we were in-

terested in determining what effect this might have on the angular variation of E_d .

In order to establish the angular dependence of the variations of the displacement threshold in a $\langle 100 \rangle$ plane, potassium knock-ons in potassium chloride moving with various energies at initial angles varying from 0° to 45° with $[100]$ were investigated. In this manner the computational threshold for the displacement of an ion (not necessarily the primary) was determined to within a few electron volts, and was seen to vary from a minimum for primary motion along $[110]$ to an indeterminate maximum in the $[100]$ direction. (No subsidiary maximum similar to that seen by Erginsoy *et al.*⁷ was observed in the $[110]$ direction. If present it may be concealed by the inherent error in our energy estimates.) Similar computations were performed for initial directions of motion not contained in the $\langle 100 \rangle$ plane, and a schematic polar plot for displacement energies in the potassium chloride lattice is given in Fig. 14. The displacement threshold for a chlorine knock-on had almost identical variation due to the similarity in size of the two ions and due to the high symmetry of the lattice.

It therefore appeared that the displacement threshold for potassium in a $\langle 110 \rangle$ direction is between 25 and 30 eV, and this conclusion was substantiated and the value roughly checked numerically by reducing the magnitude of the computational time step and repeating the run. For energies greater than 30 eV the ions of the lenses were always sufficiently perturbed to move out and be reflected by *their* barrier lenses, whence they returned to prevent the ion of the primary sequence from rejoining its lattice site after making a focusing collision. For lower energies the primary lens was only disturbed sufficiently to allow the diffusion of the ion of the sequence back to its original site, but not enough for the two lens ions to interact strongly with their own neighbors. At very low energies the initial ion was, of course, unable even to penetrate the primary barrier lens.

The threshold energy for displacement of a potassium ion directly along a $\langle 100 \rangle$ direction has not been accurately determined to lie within certain limits but is undoubtedly in excess of 150 eV, and is probably nearer to a value in the neighborhood of 200 eV. Uncertainty in this value derives from the long computational time which proved necessary to follow a typical event, beginning with an energetic impulse along or near to $\langle 100 \rangle$, to conclusion. The displacement process, moreover, was essentially different from that which took place in or near to $\langle 110 \rangle$, and was not accompanied by a string of sequential replacements. Indeed, the computations indicated the probable permanent displacement of either the primary knock-on itself or its immediate neighbor, and a large consumption of energy in the generation of $\langle 110 \rangle$ focusons in the neighboring lattice. Displacement along $\langle 111 \rangle$

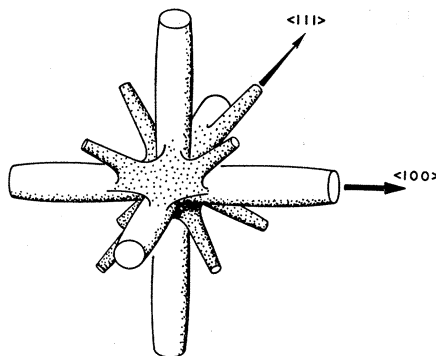


FIG. 14. Schematic polar plot of displacement threshold-energy variation with direction of motion of an ion in the potassium chloride lattice. Indeterminate maxima occur in the $\langle 100 \rangle$ and $\langle 111 \rangle$ directions, decreasing to 25–30 eV minima in $\langle 110 \rangle$ directions.

displayed a similar pattern of behavior with an indeterminate maximum threshold for ejection directly along the axis. In this case, however, the threshold falls away much more quickly with departure from axial projection—as the schematic representation of the three-dimensional displacement surface (Fig. 14) indicates. The basic pattern of the energetic events indicated in all cases the critical role of the barrier ionic lenses in determining whether or not permanent displacement occurs. The kinetics of the lens ions in relation to those of the focusing ion, and what happens *after* the focusing collision has occurred, are the influential factors once the energy for initial penetration of the barrier has been reached. The time variation of the time-dependent potential barrier, moreover, is extremely complicated, depending as it does on many-body effects, and would in all cases be impossible to predict or describe in analytical terms.

The displacement threshold for sodium in sodium chloride differed appreciably from that for chlorine. For replacement of the smaller sodium ions the assisting chlorine barriers were not greatly disturbed, and were therefore much more effective in preventing the return of the sodium ion to its lattice site. In addition, sodium-focusing collisions occurred much closer to the geometric centers of the lattice sites on account of the smaller ionic size, thereby enhancing replacement and displacement. The numerical value for the displacement threshold along the all-important $\langle 110 \rangle$ directions, for example, was as small as 20–25 eV for sodium ions, and as large as 70–90 eV for chlorine.

E. Effect of Lattice Vibrations

In the work described so far the simulated section of crystal lattice has in all instances been assumed to be at a temperature of 0°K , and zero-point motion of the ions has been neglected. Of course, this is an idealized situation, and in practice the lattice is vibrating in a system of quantized modes, whose characteristics

depend on lattice dimensions and on temperature. The simulation of realistic lattice vibrations in a calculation of the present nature would be extremely difficult and time consuming, but a qualitative approximation to the physical picture may be undertaken.

The form of the approximation we have employed is similar to that first used by Robinson and Oen,¹⁰ and assumes that the time of collision of a pair of ions is short in comparison to the vibrational period of a lattice ion. The moving ion approaching a lattice ion assumes that the latter is not, as in the zero-energy case, sitting on the lattice site, but at some position in the neighborhood. The choice of the position is made randomly by the computer from a triangular neo-Gaussian probability curve, peaked at the lattice site, and whose base size (the vibrational amplitude) and peak height are functions of temperature. Thus the moving ion first "sees" the stationary ion at a particular stage of its vibration chosen at random. While this is reasonable as a first approximation, it neglects the collective oscillations of the lattice ions, and we do not therefore have a true physical picture. Nevertheless, the approximation indicates some of the consequences of the ions' not being precisely placed on their lattice sites.

One most obvious result which one might expect would be a decrease in the efficiency of focusing, due to slight asymmetry of the lenses and the fact that it is impossible for a focuson to be carried directly along $\langle 110 \rangle$ or $\langle 111 \rangle$. Secondly, ions moving in a particular crystallographic plane will tend to be knocked out of the plane by collision with stationary ions. It was therefore decided to investigate the extent to which the pattern of damage events studied in the zero-vibration case would be affected. The event in which a potassium ion of KCl was given an energy of 80 eV at an angle of $\tan^{-1} 3/2$ to $[100]$, for example, was rerun with a thermal vibrational amplitude of $0.1 r_0$, and the trajectories were

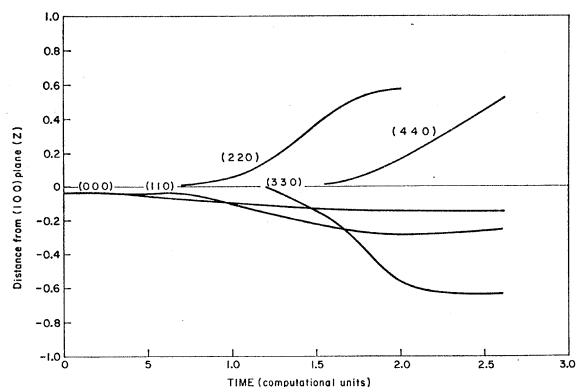


FIG. 15. Plot of distance moved perpendicular to the (100) plane in units of r_0 against time for ions of the $[110]$ focusing line in an event with the identical initial conditions to that of Fig. 3, but including the finite-temperature approximation. A decrease in focused energy and in range of the focuson is a consequence.

plotted in the usual way. The difference between the zero- and finite-temperature cases was not very marked, with the exception that in the latter event the first ion in the sequence seemed to be remaining in the replacement position. The curves shown in Fig. 15 are those of distance moved *out of plane* [i.e., perpendicular to the (100) plane of projection] against time, for each ion of the $[110]$ focusing sequence. Ions are at first ejected out of the plane and later reflected from the neighboring planes. This naturally results in a decrease in the amount of energy focused down the $[110]$ line and consequently in the range of a focuson. For example, in the 80-eV event in question, the focuson energy after five lattice spacings was 14.5 eV in the finite-temperature case, as compared with an energy of 42 eV in the zero-temperature event.

V. DISCUSSION

One general result of these events in ionic crystals has been the relatively minor influence of the Coulomb contribution to the interionic potential. The soft electrostatic potential is overshadowed during the dynamic motions of the early part of an event by the hard ion-shell repulsion of the more energetic collisions. Only during the final relaxation of the lattice in regaining equilibrium does the Coulomb part of the interaction become the more influential. This of course means that the repulsive potential will play the major role in determining efficiency of focusing of energy and displacement thresholds.

Undoubtedly, the most significant result of the computations has been the influence of the neighboring ionic lenses during focusing. Analytical calculations on assisted focusing have permitted the ions of the lenses to relax with the passage of the focused ion, but have not allowed for subsequent motion of these ions or for their action on the focusing line during the relaxation period. Consequently, they cannot predict realistically the final configuration of the disturbed lattice, with particular emphasis on permanent displacement of the ions. We have noticed that in the critical energy region for ionic displacement, below about 50 eV, the path followed by an ion moving in a $\langle 110 \rangle$ direction, for example, and where it is finally located, are almost wholly dependent on its interaction with the relevant ionic lens following its focusing collision. Also, the energy limits between which focusing occurs in higher-order focusing are largely a consequence of the assisting lens geometry. To take this into account analytically would necessitate an immensely involved calculation, so that computer simulation offers an attractive approach to a more realistic model of lattice relaxation and dynamic motion.

The $\langle 110 \rangle$ replacement sequence in ionic crystals has attracted the attention of a number of workers in the

field of color-center formation,¹⁹⁻²¹ since it represents a feasible method for the removal of an ion from the immediate neighborhood of a vacancy following irradiation, so that recombination cannot subsequently occur. It is certainly possible for a negative ion to be given several electron volts of energy, either directly or through some ionization or recombination process, by incident radiation.

One mechanism for *F*-center formation by interstitial-vacancy separation which has been widely discussed does not directly involve $\langle 110 \rangle$ replacement. This process, suggested by Varley,²² predicts the ejection of a multiply ionized (and therefore positively charged) halogen ion due to its interaction with the six surrounding alkali ions. Controversy following this suggestion centered around the lifetime of the doubly-ionized particle, since once the electron-hole recombination occurs the strong repulsion ceases, and the validity of the mechanism has been questioned mainly from this standpoint of lifetime.²³⁻²⁵ We have investigated the model by means of computer simulation, assuming a reasonable theoretical lifetime for the ionized state, and our results counteract the Varley mechanism.¹² Motion of the ionized particle takes place mainly along $\langle 110 \rangle$ and $\langle 111 \rangle$, but no replacement occurs, and after recombination the ion settles down in its own lattice site.

Pooley²¹ has suggested an alternative *F*-center production mechanism in alkali halides which depends on the separation of the vacancy and interstitial through a $\langle 110 \rangle$ replacement sequence following radiationless electron-hole recombination. To test the feasibility of the mechanism, Pooley set up a one-dimensional computer simulation of a $[110]$ line of negative ions. Neighboring lines were represented by a periodic potential field acting on ions of the central line, and the model allowed for polarization and dielectric effects. This computation produced a value for ionic displacement threshold in a number of alkali halides which was in the region of 4 or 5 eV, which implies that permanent displacements may be produced by energies arising from electron-hole recombination. The interionic potential employed by Pooley was similar to that used by ourselves, suggesting that the difference in the $\langle 110 \rangle$ displacement threshold energies (25 and 5 eV) arises from another source. To check whether any part of the difference might be due to *small* differences in potential, however, we reran several of our computations using Pooley's Born-Mayer-Verwey interaction, with no significant alteration in the results. We therefore conclude that

the differences are another consequence of the important effect of the changes in the ionic lenses. The substitution of neighboring $[110]$ lines by a periodic potential allows for the relaxation of the lenses following the passage of the traversing ion, but takes no account of the consequences of this relaxation on the interaction of the lens ions with the returning ion of the central line. Consequently, since the ionic lens does not alter in strength in the one-dimensional simulation, the return of the struck ion is hindered and it remains on a replacement site. Thus if the ion possesses initially enough energy to pass through the potential barrier (about 5 eV), it will inevitably be permanently displaced. In the three-dimensional model the complicated interaction of the returning ion of the focusing line with the moving ions of the lens results in the return of this ion to its own site if the energy is less than about 25 eV. We are of the opinion that the true threshold for production of a permanent displaced ion, not necessarily the primary knock-on, is well in excess of 5 eV, and on account of the ionic-lens influence is likely to exceed 20 eV. Interstitial-vacancy separation at very low energies through ionic-replacement sequences, with the subsequent formation of an *F* center, therefore seems unlikely. Other suggestions for color-center production mechanisms provide for the formation of neutral atoms or molecules,^{19,20} and the participation of these in replacement sequences through positive-hole tunneling. These are probably more feasible than the simple ionic case, though we have no satisfactory method of testing them with the computational method.

Another consequence of the ionic potential-barrier lenses has been revealed in the study of $\langle 112 \rangle$ and higher-order focusing, where a lower energy limit for focusing is evidently imposed by the asymmetry of the lens. The solid angle permitted for ions moving in this direction to generate a true focus is small, however, and while investigations of the $\langle 112 \rangle$ directions introduced a new type of focusing, the efficiency of the mechanism in this direction appears to be quite small. Kelly and co-workers²⁶ have reported results of sputtering experiments on potassium-chloride crystals and mention the $\langle 111 \rangle$ and $\langle 112 \rangle$ directions as the principal directions for ion emission from their crystals. The interpretation of these results in terms of directional effects *inside* the crystal is doubtful, since the extent to which the phenomenon of *focusing* is responsible for the appearance of preferential sputtering directions from crystal surfaces is presently in some dispute.^{27,28} Our computer simulations would tend to predict that $\langle 111 \rangle$ focusing has a good probability, but that $\langle 112 \rangle$ focusing is

¹⁹ C. C. Klick, Phys. Rev. **120**, 760 (1960).

²⁰ F. E. Williams, Phys. Rev. **126**, 70 (1962).

²¹ D. Pooley, Proc. Phys. Soc. (London) **87**, 245 (1966); **87**, 257 (1966), and private communication.

²² J. H. O. Varley, Nature **174**, 886 (1954).

²³ R. E. Howard and R. Smoluchowski, Phys. Rev. **116**, 314 (1959).

²⁴ D. L. Dexter, Phys. Rev. **118**, 934 (1960).

²⁵ R. E. Howard, S. Vosko, and R. Smoluchowski, Phys. Rev. **122**, 1406 (1961).

²⁶ J. C. Kelly and M. C. E. Peterson, Phys. Letters **22**, 295 (1966).

²⁷ D. E. Harrison, Jr., J. P. Johnson, III, and N. S. Levy, Appl. Phys. Letters **8**, 33 (1966).

²⁸ C. Lehmann and P. Sigmund, Phys. Status Solidi **16**, 507 (1966).

unlikely to be marked, especially for energies under 100 eV, which is the regime of energy for ions ejected in this direction during the sputtering experiment on potassium chloride. At these low energies the ion-shell repulsion collisions with the asymmetric ionic lens will cause rapid defocusing. The repulsive term in the interionic potential is predominant during the actual collision, and this fact takes precedence over any beneficial influence of Coulomb interaction with the asymmetric lens as a whole.

VI. CONCLUSION

Within the confines of the limits imposed by the computational model the progress of displacement and subdisplacement radiation damaging events in crystal-lites of pseudo-simple cubic potassium and sodium chloride follows a similar pattern to that which has been reported for fcc copper and bcc α -iron^{6,7}:

(1) Damage at low energies consists of vacancies and interstitials. At threshold energies the nature of the displacement process is strongly dependent on directional effects imposed by the lattice. At sub-threshold energies focuson propagation occurs in $\langle 100 \rangle$, $\langle 110 \rangle$, and $\langle 111 \rangle$ directions.

(2) Vacancies are of the conventional character for alkali halides, but alkali and halide ions in both salts prefer the configuration of a static crowdion along $\langle 110 \rangle$.

(3) The $\langle 110 \rangle$ directions are favored directions for the removal of energy from the vicinity of a primary event over a wide range of primary knock-on energies. At above-threshold energies a classical $\langle 110 \rangle$ assisted focuson is accompanied by a replacement sequence.

(4) The $\langle 100 \rangle$ directions permit the generation of a simple focuson, but the energy-transfer process is very inefficient.

(5) The $\langle 111 \rangle$ directions are favored for strongly assisted focuson generation since they present two triangular and symmetrical ionic lenses. At energies in excess of 100 eV, $\langle 111 \rangle$ focusons are accompanied by the generation of $\langle 110 \rangle$ focusons at angles to the initial sequence.

(6) For higher-index crystal directions, such as $\langle 112 \rangle$, the asymmetry of the ionic lenses which a sequence has to traverse introduces a new kind of focuson for which there is a lower energy limit. At energies above this limit the trajectory of the initial struck ion may be barely modified by the collision with the asymmetric lens and an impulse focuson may flow down the high-index direction. The lower limit of energy for impulse focuson generation increases with the index of the crystallographic direction.

(7) In sodium chloride the small size of the cation can

in certain circumstances allow the simultaneous generation of channelons and focusons.

(8) The displacement threshold has a minimum along or near to the $\langle 110 \rangle$ direction for both salts. The threshold is of the order of 25–30 eV for potassium chloride (potassium and chlorine) and varies between 20 eV (sodium) and 90 eV (chlorine) for sodium chloride. In all cases a dynamic crowdion action produces interstitials (static crowdions) at some distance from the site of a primary event, and a vacancy close to that site.

(9) The displacement threshold has an unknown maximum in excess of 150 eV along or near to the $\langle 100 \rangle$ or $\langle 111 \rangle$ directions.

(10) The phenomenon of displacement and replacement in the all-important $\langle 110 \rangle$ directions is very strongly dependent on the *dynamic* behavior of the disturbed $\langle 110 \rangle$ ionic lenses. This could account for the failure of arguments based on *static* considerations to explain the formation of color centers after ionizing radiation.

(11) Agitations following damage events bear some resemblance to thermal spikes as they are conventionally understood, but focuson and dynamic crowdion generation along selective low-index crystallographic directions imposes a detailed structure on the cubic symmetry of the spike.

(12) A simple model for the effect of lattice vibrations indicates little effect on the progress of a typical damaging event or on the final defect configuration, though focusons are attenuated more strongly.

(13) The long-range Coulomb part of the potential is not of such importance for interactions during a radiation damage event between ions which are separated by two or more lattice parameters, as might have been thought.

ACKNOWLEDGMENTS

We are grateful to Professor F. P. Bowden, of the Cavendish Laboratory, Cambridge for his constant interest and encouragement, to the Director of the Cambridge University Mathematical Laboratory for permission to use the Titan computer, and to the Science Research Council (United Kingdom) for a research grant and a senior fellowship (I. McC. T.), during the first part of this program. It is a pleasure to acknowledge the participation of D. Vernon Morgan of Cavendish Laboratory, Cambridge in many helpful discussions during the course of the work, and Stephen T. Imrich, Jr., of this laboratory for valuable assistance in translating the computer program. In addition, we thank the staff of the Data Processing section of North American Aviation's Rocketdyne Division for the use of their computing facilities.